



OPEN *ETFDH* mutation involves excessive apoptosis and neurite outgrowth defect via Bcl2 pathway

Chuang-Yu Lin^{1,7}, Wen-Chen Liang^{2,4,5,8}✉, Yi-Chen Yu¹, Shin-Cheng Chang², Ming-Chi Lai⁶✉ & Yuh-Jyh Jong^{2,3,5}

The most common mutation in southern Chinese individuals with late-onset multiple acyl-coenzyme A dehydrogenase deficiency (MADD; a fatty acid metabolism disorder) is c.250G > A (p.Ala84Thr) in the electron transfer flavoprotein dehydrogenase gene (*ETFDH*). Various phenotypes, including episodic weakness or rhabdomyolysis, exercise intolerance, and peripheral neuropathy, have been reported in both muscular and neuronal contexts. Our cellular models of MADD exhibit neurite growth defects and excessive apoptosis. Given that axonal degeneration and neuronal apoptosis may be regulated by B-cell lymphoma (BCL)-2 family proteins and mitochondrial outer membrane permeabilization through the activation of proapoptotic molecules, we measured the expression levels of proapoptotic BCL-2 family proteins (e.g., BCL-2-associated X protein and p53-upregulated modulator of apoptosis), cytochrome c, caspase-3, and caspase-9 in NSC-34 cells carrying the most common *ETFDH* mutation. The levels of these proteins were higher in the mutant cells than in the wide-type cells. Subsequent treatment of the mutant cells with coenzyme Q10 downregulated activated protein expression and mitigated neurite growth defects. These results suggest that the activation of the BCL-2/mitochondrial outer membrane permeabilization/apoptosis pathway promotes apoptosis in cellular models of MADD and that coenzyme Q10 can reverse this effect. Our findings aid the development of novel therapeutic strategies for reducing axonal degeneration and neuronal apoptosis in MADD.

Keywords Multiple acyl-coenzyme A dehydrogenase deficiency, Riboflavin, Carnitine, Coenzyme Q10, *ETFDH*, Apoptosis, Bcl-2, MOMP, Neuropathy

Abbreviations

MADD	Multiple acyl-coenzyme A dehydrogenase deficiency
ETF	Electron transfer flavoprotein
ETF-QO	ETF ubiquinone oxidoreductase
MOMP	mitochondrial outer membrane permeabilization
ROS	reactive oxidative species
WT	Wild-type

Multiple acyl-coenzyme A dehydrogenase deficiency (MADD; Online Mendelian Inheritance in Man [OMIM] ID: 231680), also known as glutaric aciduria type II, is a rare hereditary disorder that results from defective electron transfer and flavin homeostasis. Predominant MADD-associated genes include electron transfer flavoprotein (ETF) subunit A (OMIM ID: 608053), ETF subunit B (OMIM ID: 130410), and ETF dehydrogenase (*ETFDH*; OMIM ID: 231675), which encode ETF alpha subunit (ETFA), ETF beta subunit (ETFB), and ETF ubiquinone oxidoreductase (ETF-QO), respectively^{1–5}. MADD exhibits diverse clinical phenotypes. The mutations of *ETFDH* gene were reported to be the major cause of MADD, which often cause a late-onset

¹Department of Biomedical Science and Environmental Biology, Kaohsiung Medical University, Kaohsiung, Taiwan. ²Departments of Pediatrics, Kaohsiung Medical University Hospital, Kaohsiung Medical University, Kaohsiung, Taiwan. ³Department of Laboratory Medicine, Kaohsiung Medical University Hospital, Kaohsiung Medical University, Kaohsiung, Taiwan. ⁴Department of Pediatrics, School of Medicine, College of Medicine, Kaohsiung Medical University, Kaohsiung, Taiwan. ⁵Graduate Institute of Clinical Medicine, College of Medicine, Kaohsiung Medical University, Kaohsiung, Taiwan. ⁶Department of Pediatrics, Chi-Mei Medical Center, Tainan, Taiwan. ⁷Regenerative Medicine and Cell Therapy Research Center, Kaohsiung Medical University, Kaohsiung, Taiwan. ⁸Department of Pediatrics, Kaohsiung Medical University Hospital, Kaohsiung Medical University, Kaohsiung, Taiwan. ✉email: wen.chen.liang@gmail.com; vickylai621@gmail.com

milder phenotype characterized by episodic weakness, recurrent rhabdomyolysis, hepatomegaly, and metabolic acidosis. In addition to muscular symptoms, neurological symptoms such as leukodystrophy and peripheral neuropathy are observed in some patients^{5–11}. Encephalopathy could be present in the patients with *ETFA* or *ETFB* mutations but peripheral neuropathy was never described.

Various mechanisms have been proposed to explain the pathophysiology of MADD. Flavin is crucial for the functions of ETF and ETF-QO. Therefore, impaired binding of flavin with mutant ETF-QO, which disrupts the chaperone-mediated folding, oligomerization, and conformational stabilization of ETF-QO, may contribute to MADD. Increasing flavin concentration may partially restore protein stability and enzyme activity in the fibroblasts of patients with MADD; this observation is consistent with the findings of studies reporting that high-dose riboflavin (vitamin B2) supplementation improves the clinical and metabolic phenotypes of MADD in some patients, primarily those carrying *ETFDH* mutations^{12–17}. The disruption of flavin adenine dinucleotide homeostasis may contribute to the development of riboflavin-responsive MADD in mouse and cellular models¹⁸. However, only one study conducted using a zebrafish model carrying *EFFDH* mutations demonstrated that aberrant neural proliferation and reduced neuromuscular synapse counts are associated with metabolic dysfunction¹⁹.

Axonal degeneration and neuronal apoptosis are regulated by BCL-2 family proteins and mitochondrial outer membrane permeabilization (MOMP) through the activation of proapoptotic molecules. Several neurodegenerative diseases characterized by axonal degeneration and neuronal apoptosis have been associated with the aforementioned signaling pathway. The selective deletion of proapoptotic BCL-2 family proteins, such as BCL-2-associated X protein (Bax), delays or prevents disease onset in cellular and animal models^{20–22}. Glutamic acid, an intermediate metabolite accumulated in cells with MADD, induces neuronal damage, partially through the apoptotic pathway, in primary striatal neurons²³. We previously demonstrated that the c.250G>A (p.Ala84Thr) mutation in *ETFDH*—the most common mutation in the southern Chinese population—can cause neurite growth defects, which are ameliorated by mitochondrial cofactors, such as coenzyme Q10^{24–26}. However, the occurrence of apoptosis and the mechanisms underlying neurite growth defects in MADD remain to be explored. In the present study, we investigated the signaling pathway involved in neural defects in MADD.

Materials and methods

Cell line and transfection

Human wild-type (WT) *ETFDH* cDNA (based on the sequence of NM_004453) was cloned into the *Asi*SI and *Xho*I sites of the pCMV6-Entry vector (OriGene Technologies, US). The c.250G>A (p.Ala84Thr) point mutation construct was manufactured by GenDiscovery Biotechnology²⁶. Lentiviral vector constructs for the WT gene and the mutant gene (pLAS2w.ETFDH-Myc-DDK.Ppuro) were subcloned (at the *Nhe*I and *Eco*RI sites) into the pLAS2w.ETFDH-Myc-DDK.Ppuro construct derived from the pCMV6 vector, as described. The lentivirus, lentiviral infection, and WT and mutant NSC-34 (The spinal cord × Neuroblastoma hybrid cell line) cell lines and C2C12 were established by the national RNA Technology and Gene Manipulation Core facility (NCFB, Taiwan).

Apoptosis assays

Flow cytometry

For flow cytometry, mutant and WT NSC-34 cells were trypsinized and resuspended in phosphate-buffered saline (PBS). Apoptosis assays were performed using a commercial kit (Annexin V-FAM + PI Apoptosis Detection Reagent; Croyez Bioscience, Taipei City, Taiwan). Directly conjugated fluorescent dyes were used for flow cytometry. After antibody labeling and washing, we analyzed the labeled cells by using the FACSLyric system (BD Biosciences).

Terminal deoxynucleotidyl transferase dUTP nick end labeling assay

A terminal deoxynucleotidyl transferase dUTP nick end labeling (TUNEL) assay was performed using Click-iT Plus TUNEL Assay Kits (C10617; Invitrogen) in accordance with the manufacturer's instructions. After labeling apoptotic cells, we acquired their images through confocal microscopy and calculated the percentage of apoptotic cells.

Confocal microscopy

Mutant and WT NSC-34 cells were fixed with 4% paraformaldehyde in PBS and then permeabilized with 0.2% Triton X-100 in PBS. After PBS washing, the cells were incubated with relevant primary antibodies overnight at 4 °C. On the next day, the cells were washed and subsequently incubated with corresponding fluorescent dye-conjugated secondary antibodies for 1 h at room temperature. Next, the cells were washed with PBS, and the nuclei were stained with DAPI (4',6-diamidino-2-phenylindole). The slides were mounted using mounting medium and observed by a confocal laser scanning microscope (Carl Zeiss LSM-700).

Western blotting

Mutant and WT NSC-34 cells were harvested and then lysed with radioimmunoprecipitation assay (RIPA) buffer (Genestar). The bicinchoninic acid assay was performed to measure the levels of the total proteins in each sample. The protein samples were subjected to sodium dodecyl sulfate polyacrylamide gel electrophoresis. The percentage of gel was determined on the basis of the molecular weight of the target proteins. Subsequently, the resultant protein bands were transferred onto a polyvinylidene fluoride membrane (Immobilon-P; IPVH85R; Millipore). The conventional protocol was followed for this experiment. The membrane was blocked with 5% skimmed milk and then incubated with primary antibodies overnight at 4 °C. Next, the membrane was washed

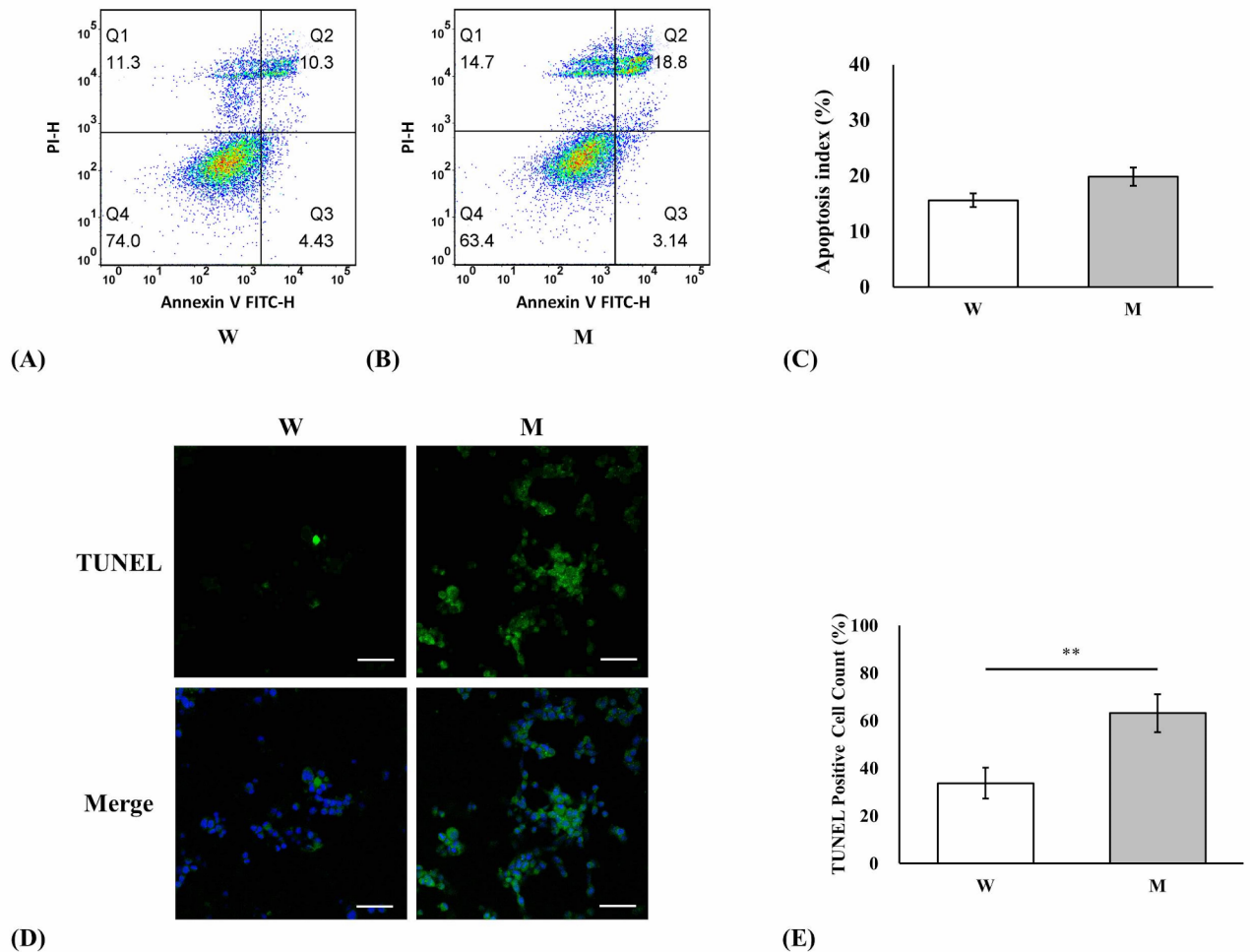


Fig. 1. The apoptosis assays. **(A: wild type and B: Mutant)** Flow cytometry showed the increased apoptosis in the mutant-type cells. In the diagram, the fourth quadrant (Q4) represents healthy living cells (FITC-/PI-), the third quadrant (Q3) represents early apoptotic cells (FITC+/PI-), the second quadrant (Q2) represents late apoptotic cells (FITC+/PI+), and the first quadrant (Q1) represents dead cells. **(C)** the cell apoptosis index of wild type and mutant cells. Apoptosis index (%) = early apoptosis rate (Q3) + late apoptosis rate (Q2). ($n = 2$). **(D)** The TUNEL stain was performed to detect the apoptotic cells. The scale bar is 50 μm in length. **(E)** The TUNEL positive cell counts of the wild type cells and the mutant cells. $n = 11 \sim 14$. The statistical significance of the different protein expressions was estimated by two-tailed student's t-test analysis. (*: $p < 0.05$, **: $p < 0.01$, ***: $p < 0.001$).

with Tris-buffered saline containing Tween 20 and incubated with horseradish peroxidase-conjugated secondary antibodies for 1 h at room temperature. This was followed by the addition of a chemiluminescent substrate. Images were obtained using the G: Box mini multiapplication imaging system (Syngene). Antibodies against the following proteins were used for this experiment: cytochrome c (Abcam), Bax (CST), p53-upregulated modulator of apoptosis (PUMA; Abcam), caspase-3 (Abcam), caspase-9 (MBL Life Science), Foxo3a (Millipore), phospho-Foxo3a (Cell Signaling Technology), and glyceraldehyde 3-phosphate dehydrogenase (GeneTex).

Neurite measurement

To measure neurites, NSC-34 cells were seeded (density: 8×10^4 cells/well) in 10-cm dishes (Nunc). The cells were cultivated in Dulbecco's Modified Eagle Medium (Gibco) supplemented with 1% horse serum, 1% penicillin-streptomycin (Gibco), and 1% nonessential amino acid solution (Sigma) after transfection; the medium was replenished every 3 days. On day 6 after transfection, neuronal cells expressing green fluorescence protein were imaged under a fluorescence microscope (Axiovert 200; Zeiss). The length of a neurite was measured using NeuronJ, which is a plugin for ImageJ software¹⁹. A total of 100 cells were analyzed per group.

Drug treatment

WT (250G) and mutant (250 A) NSC-34 cells were separately treated with coenzyme Q10 (Sigma) or riboflavin (Sigma). Different drug dosages were selected after a thorough review of the literature; the optimal therapeutic

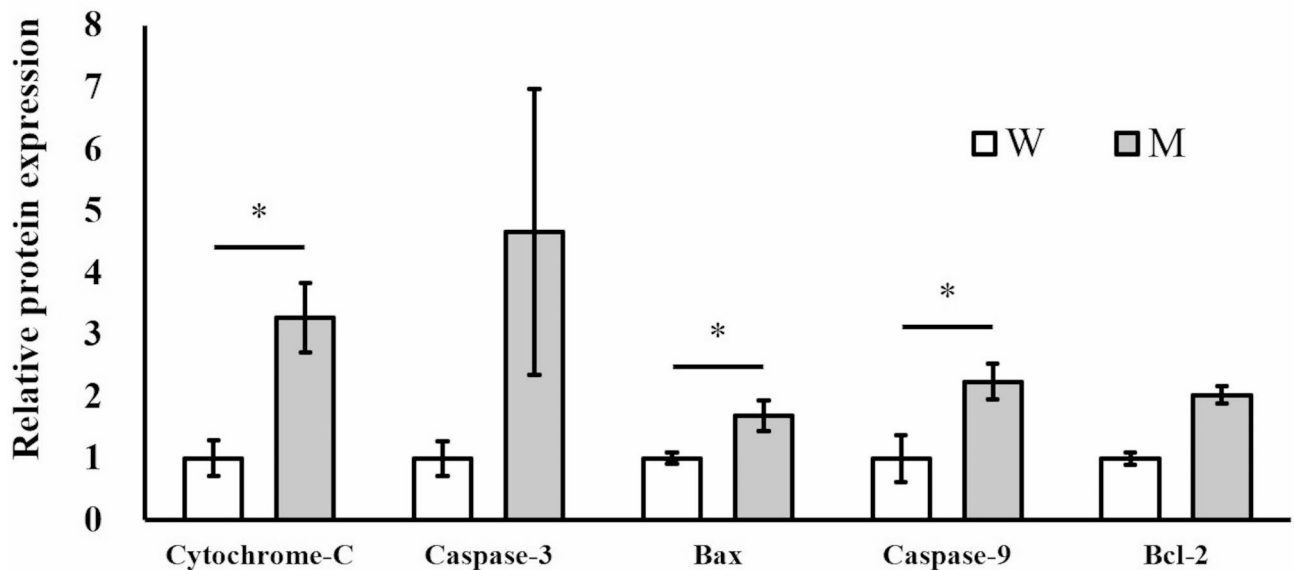


Fig. 2. The Western blotting results of relative protein expression level of wild type and mutant. Including the Cytochrome-C, Caspase-3, Bax, Caspase-9 and Bcl-2. W: *ETFDH*-250G (wild type), M: *ETFDH*-250 A (mutant type). The statistical significance of the different protein expressions was estimated by two-tailed student's *t*-test analysis. (*: $p < 0.05$, **: $p < 0.01$, ***: $p < 0.001$). $n = 2 \sim 4$.

dose was determined on the basis of dose–effect results²⁶. Neurite length was measured after 6 days of treatment. Drug-containing culture medium was replenished every 3 days.

Statistical analysis

The significance of between-group differences in protein expression levels was determined through one-way analysis of variance, followed by Tukey's honestly significant difference test. Furthermore, the significance of between-group differences in the results of apoptosis assays and of Fig. 1 for Western blotting, was determined using Student's *t* test. All analyses were performed using SPSS (version 19.0; IBM Corporation Armonk, NY, USA).

Results

Apoptosis was increased in the mutant cells

Excessive cell death was observed during cell culture, which prompted us to analyze whether apoptosis or autophagy contributed to this phenomenon. Apoptosis assays revealed that the rate of apoptosis was higher in the mutant cells than in the WT cells (Fig. 1A, B and C); however, no between-group difference was observed in the rate of autophagy (Supplement Fig. 1). The TUNEL assay revealed higher frequencies of intranuclear and intracytoplasmic dot-like staining in the mutant cells than in the WT cells (Fig. 1D and E).

BCL-2/MOMP/apoptosis pathway was activated in the mutant cells

We previously reported that NSC-34 cells carrying *ETFDH* mutations exhibit neurite growth defects²⁶. In the present study, we investigated the underlying mechanism. Our findings revealed that the BCL-2/MOMP/apoptosis pathway was activated in the mutant cells. The levels of BCL-2, Bax, cytochrome c, caspase-3, and caspase-9 were higher in the mutant cells than in the WT cells, indicating the activation of the BCL-2-regulated apoptosis pathway in the mutant cells (Fig. 2 and Supplementary Fig. 2).

Coenzyme Q10 mitigated neurite growth defects and prevented apoptosis in the mutant cells

Evidence suggests that coenzyme Q10 prevents apoptosis and promotes neuronal differentiation and neural elongation²⁷. Therefore, we investigated whether the rescue effects of coenzyme Q10 are mediated by the BCL-2/MOMP/apoptosis pathway. Coenzyme Q10 treatment helped the mutant cells overcome neurite growth defects (Fig. 3A and B). The treatment downregulated the expression of proteins associated with the activated BCL-2/MOMP/apoptosis pathway: BCL-2, Bax, cytochrome c, caspase-3, caspase-9, PUMA and pFOXO3a (Fig. 4A, B and I and Supplementary Fig. 3). Furthermore, the coenzyme Q10 treatment reduced the rate of apoptosis in the mutant cells as well (Supplementary Fig. 4).

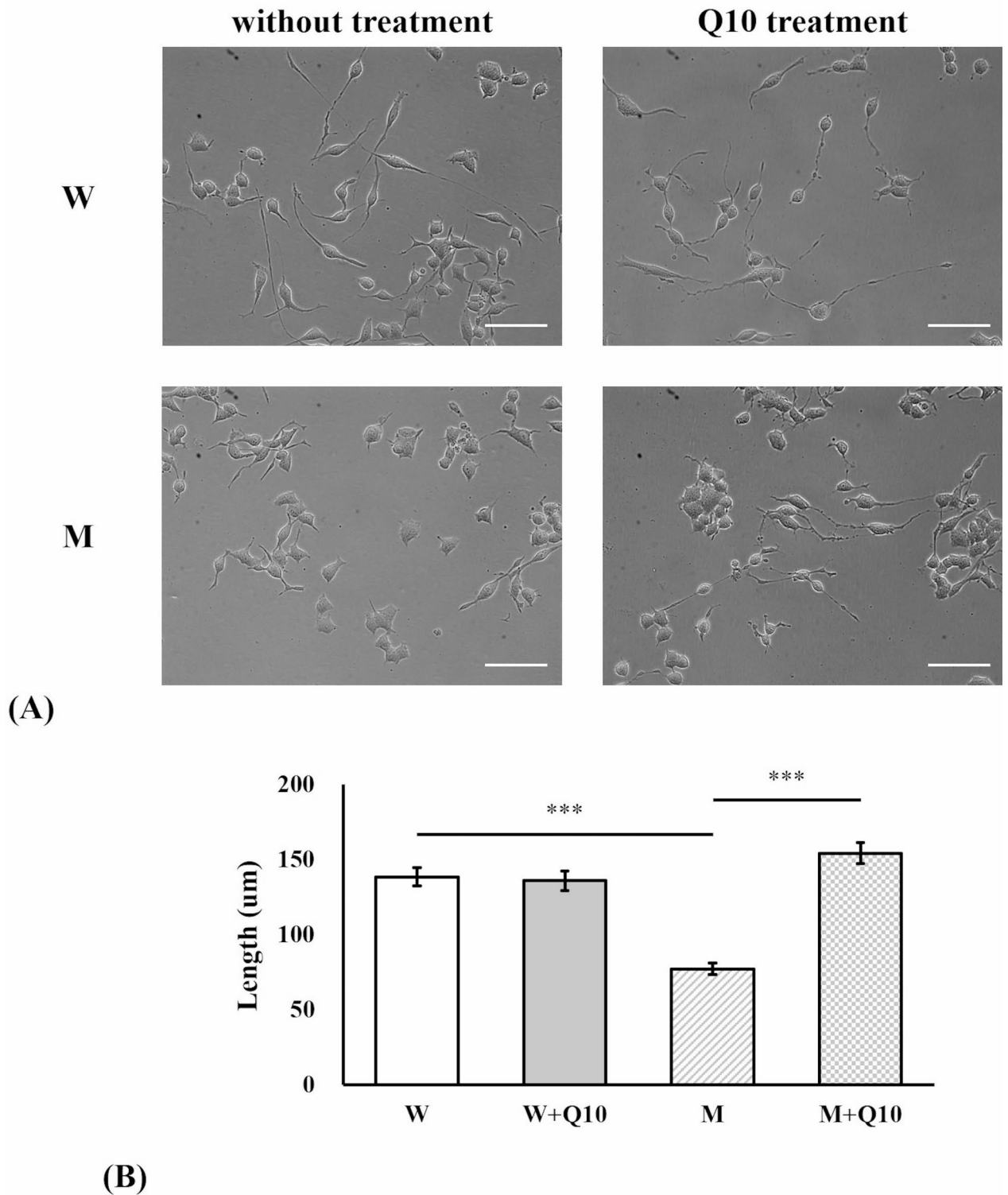


Fig. 3. The effect of neurites outgrowth by coenzyme-Q10 treatment. **(A)** the morphology of neurites in wild type and mutant cells observed by phase contrast microscopy. The scale bar is 100 μm in length. **(B)** The lengths of neurites in wild type and mutant cells with coenzyme-Q10 treatment. W: ETFDH-250G (wild type), M: ETFDH-250 A (mutant type), W + Q10: wild type treated with coenzyme Q10, M + Q10: mutant type treated with coenzyme Q10. The statistical significance of the different protein expressions was estimated by one-way analysis of variance (ANOVA) followed by Tukey's test (HSD). (*: $p < 0.05$, **: $p < 0.01$, ***: $p < 0.001$). $n = 60$.

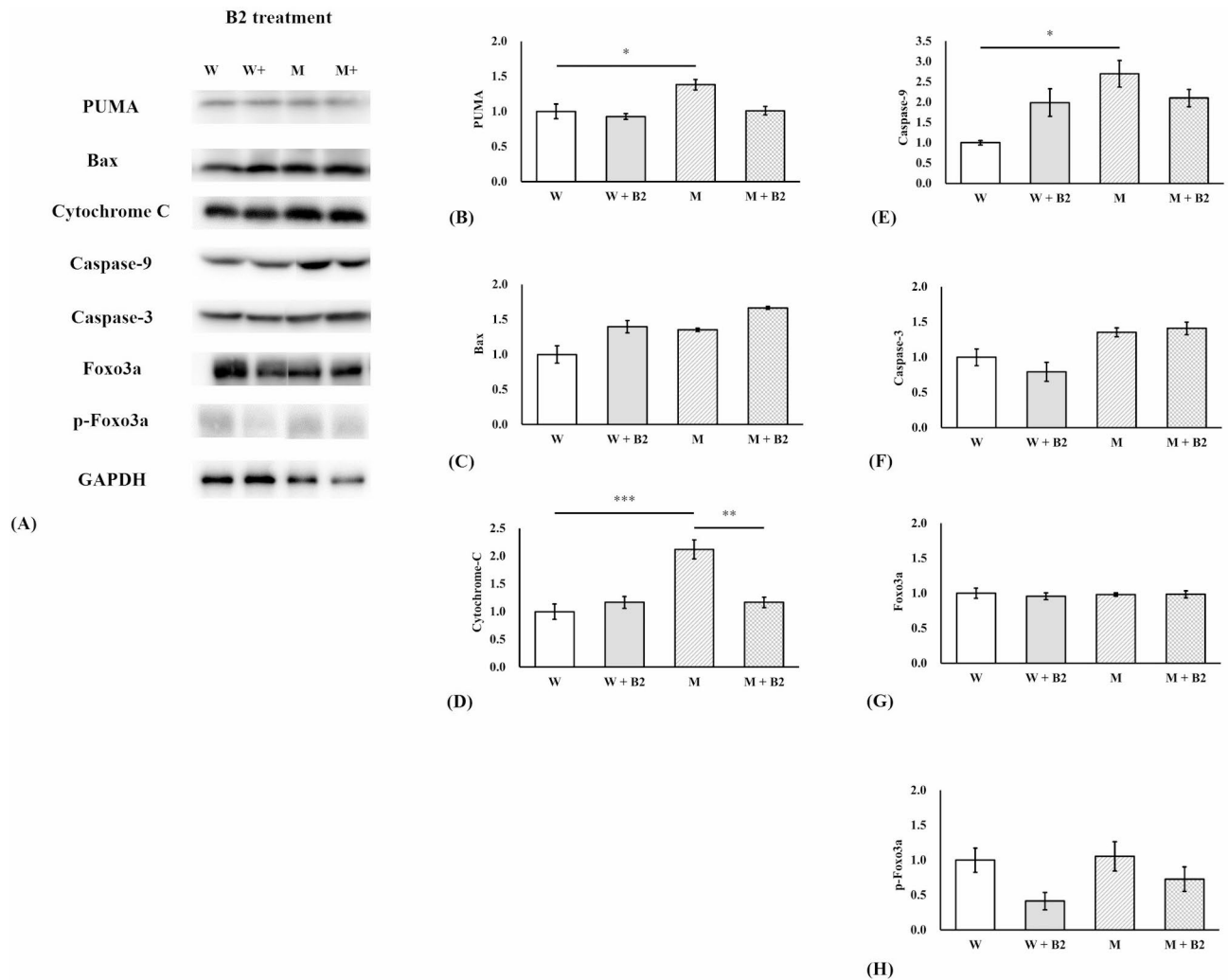


Fig. 4. The Western blotting of BCL-2 regulated apoptosis signaling pathways that treated with coenzyme Q10. **(A)** The Western blotting results including PUMA, Bax, Cytochrome-C, Caspase-9, Caspase-3, FOXO3a, p-FOXO3a and Bcl-2. W: ETFDH-250G (wild type), M: ETFDH-250 A (mutant type), W + Q10: wild type treated with coenzyme Q10, M + Q10: mutant type treated with coenzyme Q10. **(B, C, D, E, F, G, H and I)** The quantification of the Western blot results. All the protein expression levels were normalized with GAPDH expression level. The statistical significance of the different protein expressions was estimated by one-way analysis of variance (ANOVA) followed by Tukey's test (HSD). (*: $p < 0.05$, **: $p < 0.01$, ***: $p < 0.001$). $n = 2 \sim 4$.

Riboflavin treatment mitigated neurite growth defects but did not prevent apoptosis in the mutant cells

Riboflavin is effective against late-onset MADD in most patients. Researchers are increasingly interested in the therapeutic mechanisms underlying this treatment. We therefore also investigated whether riboflavin prevents apoptosis through the BCL-2/MOMP/apoptosis pathway. Similar to coenzyme Q10, riboflavin facilitated the recovery of neurite length. However, no significant reductions were noted in the expression levels of Bax, caspase-3, caspase-9, PUMA, and pFOXO3a, but not that of cytochrome c, after riboflavin treatment (Fig. 5A, B and H and Supplementary Fig. 5).

Discussion

MADD has traditionally been characterized as a metabolic myopathy presenting with muscle weakness and excessive sarcoplasmic lipid accumulation. In some patients, neural phenotypes are present in patients with MADD, manifesting as peripheral neuropathy, sensory ataxia, or Guillain-Barre-like syndrome^{6,8-11}. The nerve biopsy results of these patients revealed axonal degeneration and myelination loss¹⁰. Similarly, a zebrafish model of MADD carrying *xav* mutants exhibited pronounced neural phenotypes, such as low neuropil counts, abnormal glial patterning, diminished motor axon branching, reduced neuromuscular synaptogenesis, increased apoptosis, and progressive paralysis¹⁹. Therefore, MADD affects the peripheral nervous system. However, unlike the mechanisms underlying muscular symptoms, those underlying neural phenotypes remain unexplored.

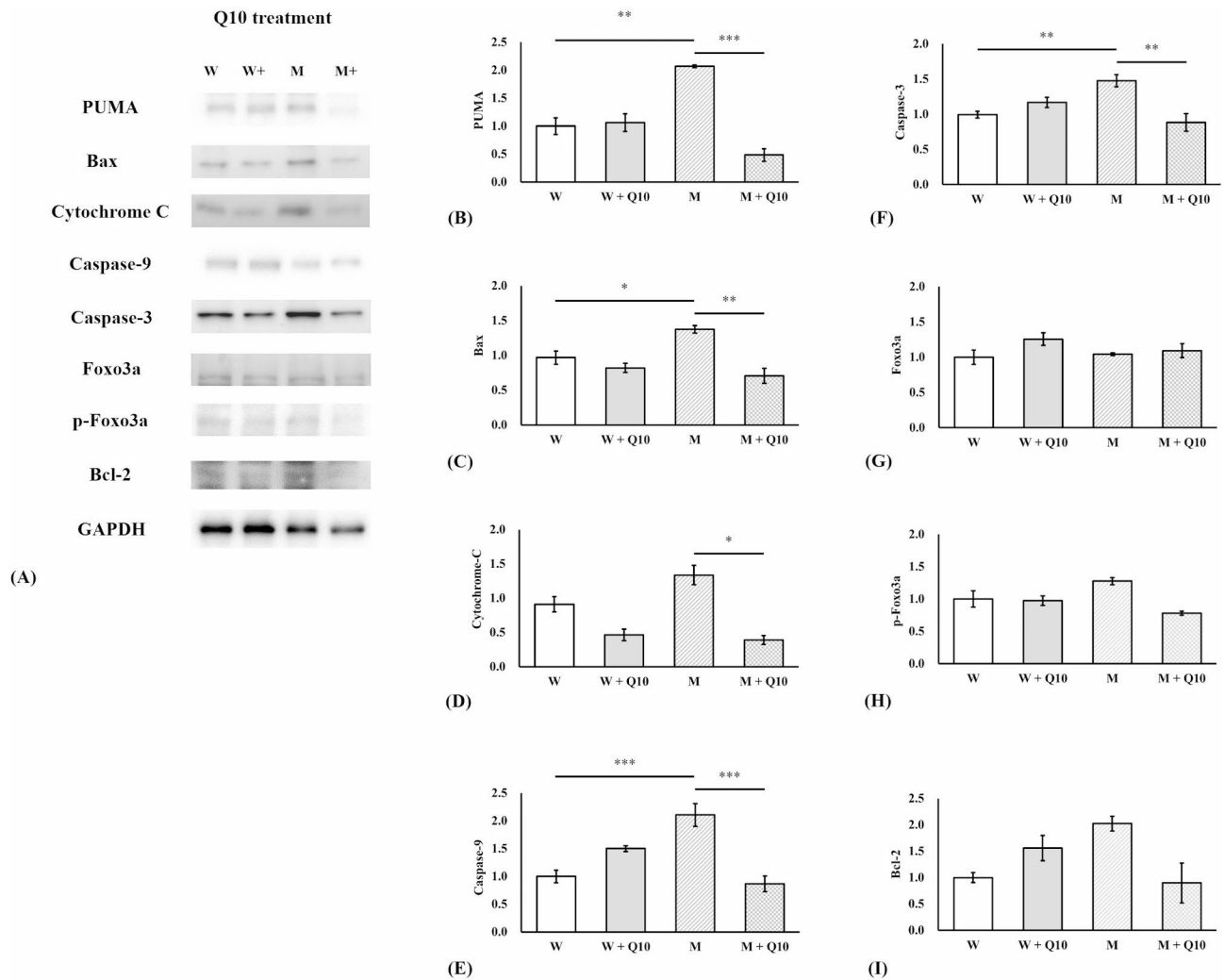


Fig. 5. The Western blotting of BCL-2 regulated apoptosis signaling pathway that treated with riboflavin (B2). (A) The Western blotting results including the PUMA, Bax, Cytochrome-C, Caspase-9, Caspase-3, FOXO3a and p-FOXO3a. W: ETFDH-250G (wild type), M: ETFDH-250 A (mutant type), W + B2: wild type treated with riboflavin (B2), M + QB2: mutant type treated with riboflavin (B2). (B, C, D, E, F, G and H) All the protein expression levels were normalized with GAPDH expression level. The statistical significance of the different protein expressions was estimated by one-way analysis of variance (ANOVA) followed by Tukey's test (HSD). (*: $p < 0.05$, **: $p < 0.01$, ***: $p < 0.001$). $n = 2 \sim 4$.

In this study, we first demonstrated apoptosis induction and neurite growth defects in the mutant cells and subsequently revealed the activation of the BCL-2/MOMP/apoptosis pathway in these cells compared with WT cells. These aspects have not been explored in previous studies. The BCL-2 family regulates not only life and death but also axonal degeneration. Mitochondria, the principal sites for energy production, are also the sites of BCL-2-protein-regulated apoptosis²⁸. Given that neurons have extended axons, the BCL-2-protein pathway appears to govern axon degeneration²⁹. Coenzyme Q10 mitigates oxidative stress and prevents apoptosis in spinal cord injury models³⁰. We previously demonstrated its efficacy in rescuing neurite growth defects resulting from *ETFDH* mutations²⁶. In the present study, we treated both mutant and WT NSC-34 cells with coenzyme Q10 to evaluate its therapeutic role and associated mechanisms. Our results revealed reductions in the proportion of TUNEL-positive cells and the expression levels of PUMA, pFOXO3a, cytochrome c, caspase-3, caspase-9, and Bax, suggesting that coenzyme Q10 prevented apoptosis in the cellular model of MADD. However, coenzyme Q10 may operate through other mechanisms in addition to the BCL-2/MOMP/apoptosis pathway. Evidence suggests that coenzyme Q10 modulates the open-close transition of the mitochondrial permeability transition pore, thereby preventing apoptosis through the inhibition of mitochondrial depolarization³¹. Another study reported that coenzyme Q10 hinders the formation of inflammasomes and the release of interleukin-1 β , rescuing cells from death due to *ETFDH* mutations; however, this study only mentioned reduced cell viability without indicating apoptosis³². Thus, our study is the first to explore apoptosis in cells carrying *ETFDH* mutations. Further studies are required to investigate additional regulatory mechanisms.

Riboflavin improves the outcomes of late-onset MADD in many patients carrying *ETFDH* mutations. However, it does not seem to regulate the BCL-2/MOMP/apoptosis pathway, as evident by the lack of an increase in the expression level of any proapoptotic protein in riboflavin-treated mutant NSC-34 cells in our study. Riboflavin plays diverse roles in flavoenzyme-mediated metabolism of lipids and proteins, and it is crucial for the energy production function of the mitochondria³³. We previously demonstrated that both coenzyme Q10 and riboflavin considerably ameliorated neurite growth defects²⁶. However, the present study suggests that coenzyme Q10 and riboflavin act through different signaling pathways to mitigate axonal degeneration. The role of riboflavin in the regulation of apoptosis is multifaceted. Although riboflavin deficiency may induce apoptosis, it may also reduce cell death by exerting antioxidative effects^{34,35}. There was also a study reporting that the combination of riboflavin and ultraviolet light can induce apoptosis³⁶. Recent study showed that the complex of ETFDH is essential for oxidative phosphorylation complex III (CIII) activity for the normal function of mitochondria in the skeletal muscle. Moreover, the complex of ETFDH, CIII and coenzyme Q2 (part of the coenzyme Q10 pathway), which guide electrons from lipid substrates to the respiratory chain can reduce electron leakage and the production of reactive oxidative species (ROS) (37). The mutation of *ETFDH* can cause malfunction of the mitochondria respiratory chain and increase the ROS to trigger the following apoptotic signaling pathway. The current literature lacks clarity on the association between riboflavin and axonal degeneration and similarly, riboflavin therapy has been reported not to recover or even improve neuropathic symptoms (11). The present study corroborates that coenzyme Q10 is more effective than riboflavin in preventing neuronal apoptosis and mitigating axonal degeneration in patients with MADD.

The key regulators and executors of apoptosis are the pro-apoptotic and pro-survival (anti-apoptotic) members of the BCL-2 family proteins. The balance between those two BCL-2 proteins members can control the cell fate between cell death and life (38). The mutation of *ETFDH* might increase the ROS, then cause the MOMP, and upregulate the production of BAX, Caspase 3/9 and Cytochrome c to trigger the apoptotic pathway eventually. The cell line used in this study (NSC-34) exhibits many motor neuron-like properties, which make it a suitable model for studying neuronal diseases^{39–41}. BCL-2 overexpression plays multifaceted roles in the regulation of apoptosis; it exerts antiapoptotic effects on rat hippocampal precursor cells, inducing neurite outgrowth⁴², and also induces axonal degeneration and apoptosis^{28,43}. Based on this study, the different roles of BCL-2 indicate that this protein participates in different pathways involved in the degeneration and regeneration of axons corresponding to the central and peripheral nervous systems, however this may require an in vivo approach system to further study the role of BCL-2 involved in neuronal pathologies of MADD. Advanced studies should also be conducted in the future to identify the roles of BCL-2 in different types of neuronal cells and clarify the interactions between Bax, the mitochondrial outer membrane, and the mitochondrial inner membrane⁴⁴.

Conclusion

Our findings indicate that the BCL-2/MOMP/apoptosis pathway mediates neurite growth defects and excessive apoptosis in cells carrying *ETFDH* mutations. Coenzyme Q10 can prevent the activation of this pathway, mitigate neurite growth defects, as well as apoptosis. These findings may facilitate the development of novel therapeutic strategies for reducing axonal degeneration and neuronal apoptosis in patients with MADD.

Data availability

All data generated or analyzed during this study are included in this published article and its supplementary information files.

Received: 23 March 2024; Accepted: 3 October 2024

Published online: 25 October 2024

References

- Indo, Y., Glassberg, R., Yokota, I. & Tanaka, K. Molecular characterization of variant alpha-subunit of electron transfer flavoprotein in three patients with glutaric acidemia type II—and identification of glycine substitution for valine-157 in the sequence of the precursor, producing an unstable mature protein in a patient. *Am. J. Hum. Genet.* **49**, 575–580 (1991).
- Freneaux, E., Sheffield, V. C., Molin, L., Shires, A. & Rhead, W. J. Glutaric acidemia type II. Heterogeneity in beta-oxidation flux, polypeptide synthesis, and complementary DNA mutations in the alpha subunit of electron transfer flavoprotein in eight patients. *J. Clin. Invest.* **90**, 1679–1686 (1992).
- Beard, S. E., Goodman, S. I., Bemelen, K. & Freman, F. E. Characterization of a mutation that abolishes quinone reduction by electron transfer flavoprotein-ubiquinone oxidoreductase. *Hum. Mol. Genet.* **4**, 157–161 (1995).
- Goodman, S. I., Binard, R. J., Woontner, M. R. & Freman, F. E. Glutaric acidemia type II: gene structure and mutations of the electron transfer flavoprotein:ubiquinone oxidoreductase (ETF:QO) gene. *Mol. Genet. Metab.* **77**, 86–90 (2002).
- Ghisla, S. & Thorpe, C. Acyl-CoA dehydrogenases. A mechanistic overview. *Eur. J. Biochem.* **271**, 494–508 (2004).
- Van Hove, J. L. K. et al. D,L-3-hydroxybutyrate treatment of multiple acyl-CoA dehydrogenase deficiency (MADD). *Lancet.* **361**, 1433–1435 (2003).
- Ishii, K. et al. Central nervous system and muscle involvement in an adolescent patient with riboflavin responsive multiple acyl-CoA dehydrogenase deficiency. *Brain Dev.* **32**, 669–672 (2010).
- Wang, Z. et al. Severe sensory neuropathy in patients with adult-onset multiple acyl-CoA dehydrogenase deficiency. *Neuromuscul. Disord.* **26**, 170–175 (2016).
- Hong, D., Yu, Y., Wang, Y., Xu, Y. & Zhang, J. Acute-onset multiple acyl-CoA dehydrogenase deficiency mimicking Guillain-Barré syndrome: two cases report. *BMC Neurol.* **18**, 219 (2018).
- Huang, K., Duan, H. Q., Li, Q. X., Luo, Y. B. & Yang, H. Investigation of adult-onset multiple acyl-CoA dehydrogenase deficiency associated with peripheral neuropathy. *Neuropathology.* **40**, 531–539 (2020).
- Lupica, A. et al. Diagnostic challenges in late onset multiple acyl-CoA dehydrogenase deficiency: clinical, morphological, and genetic aspects. *Front. Neurol.* **13**, 815523 (2022).

12. Gregersen, N., Christensen, M. F., Christensen, E. & Kølvraa, S. Riboflavin responsive multiple acyl-CoA dehydrogenation deficiency. Assessment of 3 years of riboflavin treatment. *Acta Paediatr. Scand.* **75**, 676–681 (1986).
13. Zhang, J., Frerman, F. E. & Kim, J. J. Structure of electron transfer flavoprotein-ubiquinone oxidoreductase and electron transfer to the mitochondrial ubiquinone pool. *Proc. Natl. Acad. Sci. U. S. A.* **103**, 16212–16217 (2006).
14. Olsen, R. K. et al. ETFDH mutations as a major cause of riboflavin-responsive multiple acyl-CoA dehydrogenation deficiency. *Brain.* **130**, 2045–2054 (2007).
15. Lucas, T. G. et al. Cofactors and metabolites as potential stabilizers of mitochondrial acyl-CoA dehydrogenases. *Biochim. Biophys. Acta.* **1812**, 1658–1663 (2011).
16. Cornelius, N. et al. Molecular mechanisms of riboflavin responsiveness in patients with ETF-QO variations and multiple acyl-CoA dehydrogenation deficiency. *Hum. Mol. Genet.* **21**, 3435–3448 (2012).
17. Angelini, C. Spectrum of metabolic myopathies. *Biochim. Biophys. Acta.* **1852**, 615–621 (2015).
18. Xu, J. et al. ETFDH mutations and flavin adenine dinucleotide homeostasis disturbance are essential for developing riboflavin-responsive multiple acyl-coenzyme A dehydrogenation deficiency. *Ann. Neurol.* **84**, 659–673 (2018).
19. Song, Y. et al. Mechanisms underlying metabolic and neural defects in zebrafish and human multiple acyl-CoA dehydrogenase deficiency (MADD). *PLoS One.* **4**, e8329. <https://doi.org/10.1371/journal.pone.0008329> (2009).
20. Gould, T. W. et al. Complete dissociation of motor neuron death from motor dysfunction by Bax deletion in a mouse model of ALS. *J. Neurosci.* **26**, 8774–8786 (2006).
21. Kumari, S., Dhapola, R. & Reddy, D. H. K. Apoptosis in Alzheimer's disease: insight into the signaling pathways and therapeutic avenues. *Apoptosis.* **28**, 943–957 (2023).
22. Risner, M. L., Pasini, S., McGrady, N. R. & Calkins, D. J. Bax contributes to retinal ganglion cell dendritic degeneration during Glaucoma. *Mol. Neurobiol.* **59**, 366–1380 (2022).
23. Tian, F. et al. Glutaric acid-mediated apoptosis in primary striatal neurons. *Biomed. Res. Int.* **484731** (2014). (2014).
24. Liang, W. C. et al. ETFDH mutations, CoQ10 levels, and respiratory chain activities in patients with riboflavin-responsive multiple acyl-CoA dehydrogenase deficiency. *Neuromuscul. Disord.* **19**, 212–216 (2009).
25. Wang, Z. Q., Chen, X. J., Murong, S. X., Wang, N. & Wu, Z. Y. Molecular analysis of 51 unrelated pedigrees with late-onset multiple acyl-CoA dehydrogenation deficiency (MADD) in southern China confirmed the most common ETFDH mutation and high carrier frequency of c.250G > A. *J. Mol. Med. (Berl).* **89**, 569–576 (2011).
26. Liang, W. C. et al. Neurite growth could be impaired by ETFDH mutation but restored by mitochondrial cofactors. *Muscle Nerve.* **56**, 479–485 (2017).
27. Nakamura, A. et al. Cellular level of coenzyme Q increases with neuronal differentiation, playing an important role in neural elongations. *J. Clin. Biochem. Nutr.* **71**, 89–96 (2022).
28. Kale, J., Osterlund, E. J. & Andrews, D. W. BCL-2 family proteins: changing partners in the dance towards death. *Cell. Death Differ.* **25**, 65–80 (2018).
29. Misgeld, T. & Schwarz, T. L. Mitostasis in neurons: maintaining mitochondria in an extended cellular architecture. *Neuron.* **96**, 651–666 (2017).
30. Li, X. et al. Coenzyme Q10 suppresses oxidative stress and apoptosis via activating the Nrf-2/NQO-1 and NF- κ B signaling pathway after spinal cord injury in rats. *Am. J. Transl. Res.* **11**, 6544–6552 (2019).
31. Papucci, L. et al. Coenzyme Q10 prevents apoptosis by inhibiting mitochondrial depolarization independently of its free radical scavenging property. *J. Biol. Chem.* **278**, 28220–28228 (2003).
32. Chokchaiwong, S. et al. Coenzyme Q10 serves to couple mitochondrial oxidative phosphorylation and fatty acid β -oxidation, and attenuates NLRP3 inflammasome activation. *Free Radic Res.* **52**, 1445–1455 (2018).
33. Mosegaard, S. et al. Riboflavin deficiency-implications for general human health and inborn errors of metabolism. *Int. J. Mol. Sci.* **21**, 3847 (2020).
34. Zhang, B. et al. Riboflavin (vitamin B2) deficiency induces apoptosis mediated by endoplasmic reticulum stress and the CHOP pathway in HepG2 cells. *Nutrients.* **14**, 3356 (2022).
35. Olfat, N., Ashoori, M. & Saedisomeolia, A. Riboflavin is an antioxidant: a review update. *Br. J. Nutr.* **128**, 1887–1895 (2022).
36. Hu, H. et al. Apoptosis as an underlying mechanism in lymphocytes induced by riboflavin and ultraviolet light. *Transfus. Apher. Sci.* **59**, 102899 (2020).
37. Herrero Martin, J. C. et al. An ETFDH-derived metabolon supports OXPHOS efficiency in skeletal muscle by regulating coenzyme Q homeostasis. *Nat. Metabolism.* **6**, 209–225 (2024).
38. Singh, R., Letai, A. & Sarosiek, K. Regulation of apoptosis in health and disease: the balancing act of BCL-2 family proteins. *Nat. Rev.* **20**, 175–193 (2019).
39. Cashman, N. R. et al. Neuroblastoma x spinal cord (NSC) hybrid cell lines resemble developing motor neurons. *Dev. Dyn.* **194**, 209–221 (1992).
40. Pfeiffer-Guglielmi, B. & Jansen, R. P. The motor neuron-like cell line NSC-34 and its parent cell line N18TG2 have glycogen that is degraded under cellular stress. *Neurochem Res.* **46**, 1567–1576 (2021).
41. Matusica, D., Fenech, M. P., Rogers, M. L. & Rush, R. A. Characterization and use of the NSC-34 cell line for study of neurotrophin receptor trafficking. *J. Neurosci. Res.* **86**, 553–565 (2008).
42. Lee, Y. Y. et al. Bcl-2 overexpression induces neurite outgrowth via the Bmp4/Tbx3/NeuroD1 cascade in H19-7 cells. *Cell. Mol. Neurobiol.* **40**, 153–166 (2020).
43. Pemberton, J. M., Pogmore, J. P. & Andrews, D. W. Neuronal cell life, death, and axonal degeneration as regulated by the BCL-2 family proteins. *Cell. Death Differ.* **28**, 108–122 (2021).
44. Kalkavan, H. & Green, D. R. MOMP, cell suicide as a BCL-2 family business. *Cell. Death Differ.* **25**, 46–55 (2018).

Acknowledgements

The authors thank the Center for Research Resources and Development in Kaohsiung Medical University for the assistance in flow cytometry and confocal image analysis. This study was supported by the grants of 108CM-KMU-08 and KMUH-106-6R46.

Author contributions

C.-Y.L., W.-C.L. and M.-C.L. conceptualized this study; C.-Y.L., Y.-C.Y. and S.-C.C. performed experiments and collected data for analysis; C.-Y.L., W.-C.L., M.-C.L. and Y.-J.J. wrote the draft and performed the paper review and editing; All authors have read and agreed to the published version of the manuscript.

Declarations

Competing interests

The authors declare no competing interests.

Disclosure

All authors disclose no conflicts related to this study.

Additional information

Supplementary Information The online version contains supplementary material available at <https://doi.org/10.1038/s41598-024-75286-4>.

Correspondence and requests for materials should be addressed to W.-C.L. or M.-C.L.

Reprints and permissions information is available at www.nature.com/reprints.

Publisher's note Springer Nature remains neutral with regard to jurisdictional claims in published maps and institutional affiliations.

Open Access This article is licensed under a Creative Commons Attribution-NonCommercial-NoDerivatives 4.0 International License, which permits any non-commercial use, sharing, distribution and reproduction in any medium or format, as long as you give appropriate credit to the original author(s) and the source, provide a link to the Creative Commons licence, and indicate if you modified the licensed material. You do not have permission under this licence to share adapted material derived from this article or parts of it. The images or other third party material in this article are included in the article's Creative Commons licence, unless indicated otherwise in a credit line to the material. If material is not included in the article's Creative Commons licence and your intended use is not permitted by statutory regulation or exceeds the permitted use, you will need to obtain permission directly from the copyright holder. To view a copy of this licence, visit <http://creativecommons.org/licenses/by-nc-nd/4.0/>.

© The Author(s) 2024